Dielectric relaxation in o-TaS_3: Charge-density-wave screening and near-commensurability effects

W. G. Lyons and J. R. Tucker
Department of Electrical and Computer Engineering and Coordinated Science Laboratory, University of Illinois at Urbana-Champaign, Urbana, Illinois 61801
(Received 2 March 1989)

The temperature dependence of the rf dielectric response has been measured from 223 down to 100 K for the charge-density-wave (CDW) conductor o-TaS_3. A temperature-independent response close to the transition gives way to an Arrhenius behavior below 150 K. All features of the experimental data are quantitatively reproduced by a simple phenomenological model which includes normal-carrier screening of the CDW. Data taken below 150 K are shown to be consistent with the appearance of a second pinned mode, now identified as a universal feature associated with a temperature-activated CDW response. Near-commensurability effects are proposed to account for the observed increase in the static dielectric constant and decrease in the dc threshold field between 150 and 100 K.

The strong frequency dependence of the ac conductivity $\sigma(\omega)$ and large value of the static dielectric constant $\epsilon(\omega\rightarrow 0)\sim 10^6-10^8$ are often cited as evidence for the collective nature of charge transport in sliding-charge-density-wave (CDW) systems.[1,2] In some materials, much of the linear ac dynamics can be modeled as a simple damped oscillator.[3] The ac conductivity can then be used directly to estimate the CDW pinning frequency and inertial damping constant.[4] However, it is the dielectric response function $\epsilon(\omega)=\epsilon_0+\sigma(\omega)/i\omega$, first systematically measured on $K_{0.30}MoO_3$ ("blue bronze"),[5] that quantifies the long-wavelength CDW polarizability and its associated relaxation. If the ac amplitude of the probe signal is kept below several percent of the dc threshold field,[6-8] a well-defined static dielectric constant is obtained. In general, the dielectric response can exhibit complex, temperature-dependent behavior. Here we demonstrate that this behavior can be interpreted in terms of a simple phenomenological model, showing good quantitative agreement with extensive measurements on o-TaS_3 crystals.

A physical picture of CDW polarization naturally begins with the Ginzburg-Landau description of Fukuyama, Lee, and Rice (FLR).[9] Building on FLR, a phenomenological model based on strong impurity pinning was recently proposed,[10] treating several aspects of the CDW polarization. When CDW polarization occurs over a length scale L along the chain direction, the static dielectric constant is approximately given by

$$\epsilon(\omega\rightarrow 0)\approx\frac{e^2L^2}{6\pi\hbar v_F A_0}\approx\frac{n_c e^2}{M_F\omega_p^2}\ . \tag{1}$$

Here, A_0 is the cross-sectional area per conducting chain, v_F is the Fermi velocity, n_c is the condensed CDW carrier density, ω_p is an average pinning frequency, and M_F is the inertial Fröhlich mass. Within our strong impurity pinning model, large-volume and long-length-scale ($L\sim 1\ \mu$m) average phase modes dominate the CDW polarizability and dielectric response at low frequencies. The value of L is estimated to be approximately equal to the mean spacing $1/n_i A_0$ between impurities along a single conducting chain, where n_i is the impurity concentration. These large-volume modes represent the deformable motion of the CDW, and therefore require normal carrier screening to mediate Coulombic forces. An average dielectric relaxation time τ_0 characterizes the time needed for CDW phase relaxation toward a new configuration. The associated dielectric relaxation frequency, $\omega_0\approx 1/\tau_0$, has a direct analogy with the "crossover frequency" $\omega_{CO}=\omega_p^2\tau_i$ marking the rise in $\sigma(\omega)$ for a simple overdamped oscillator, where τ_i represents the intrinsic CDW damping. As the normal carrier concentration is reduced in fully gapped materials at low temperature, however, an activated damping $\tau_A\sim\exp(-\Delta/k_BT)$ due to normal carrier screening effects will eventually dominate the intrinsic damping of the CDW system. Once this occurs, the large-volume average phase modes are driven to low frequencies, $\omega_0\approx\sigma_n(T)/\epsilon(\omega\rightarrow 0)$, and a second mode with a higher pinning frequency ω_p' appears. This millimeter-wave mode at ω_p' is the one traditionally associated with strong pinning on the volume scale n_i^{-1} of a single impurity, and it represents a universal feature in CDW systems with a temperature-activated response.[11]

Measurements were made on nominally pure o-TaS_3 crystals from the transition temperature, 223 K, down to 100 K in an open-cycle Janis Supertran equipped for rf measurements. Data were taken with a Polarad ZPV network analyzer, and HP85044A reflection-transmission test set, and a Marconi 2022 rf signal generator. Small ac signal amplitudes $E_{ac}\leq 0.03E_T$ were used relative to the dc threshold E_T. The effects of metastable states were minimized by dc biasing the sample well above threshold after each change in temperature.[12] Temperature stability was also carefully controlled to within 50 mK. Gold

paste contacts were applied to the crystals, which were mounted in the usual two-probe configuration. Complex impedance analysis was used to ensure the quality of the contacts.[5] Previous studies have attempted to resolve the behavior of the dielectric response in o-TaS_3 at frequencies far below the dielectric relaxation frequency.[6,8,13] Here we have instead concentrated on the frequency region near and above the dielectric relaxation frequency as a function of temperature.

Figure 1 shows the measured ac conductivities at 150, 130, and 110 K, normalized to the reported values for the maximum ac conductivity at millimeter-wave frequencies[14] (which are all approximately equal to the room-temperature value). Also included in Fig. 1 are the millimeter-wave data on a similar crystal from Ref. 14. Figure 2 shows the dielectric response function calculated from the ac conductivity, and normalized to the measured static dielectric constant $\epsilon(\omega\rightarrow 0)$ at each temperature. The CDW response is essentially unchanged from the temperature ($\sim$200 K) at which the Peierls gap is fully developed down to 150 K. Below 150 K, a temperature-activated behavior sets in. The magnitude of the ac conductivity drops off below 1 GHz and the

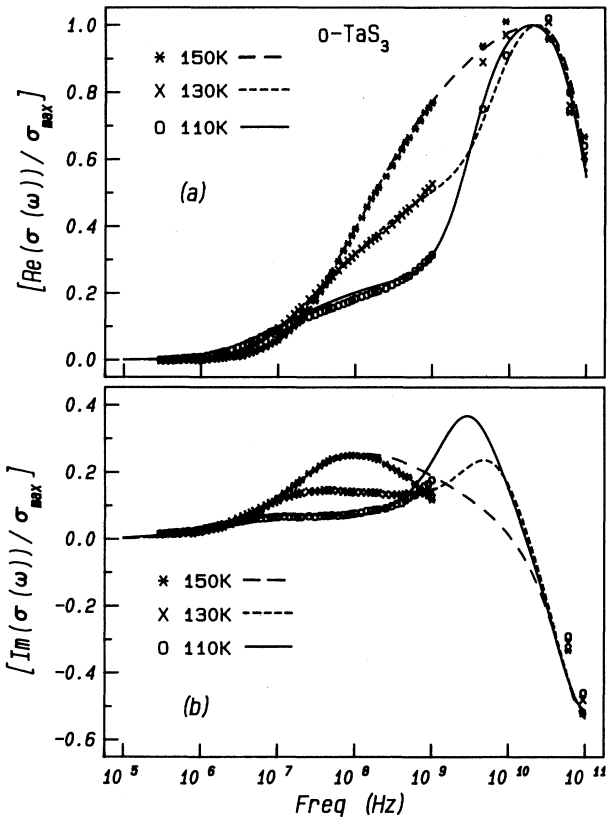

FIG. 1. Frequency-dependent ac conductivity of o-TaS_3 at 150, 130, and 110 K, normalized to reported $\sigma_{max}(T)$ values (Ref. 14). Solid and dashed lines are theoretical model predictions using Eq. (2) and the parameters listed in Table I. High-frequency data points above 1 GHz are taken from Ref. 14.

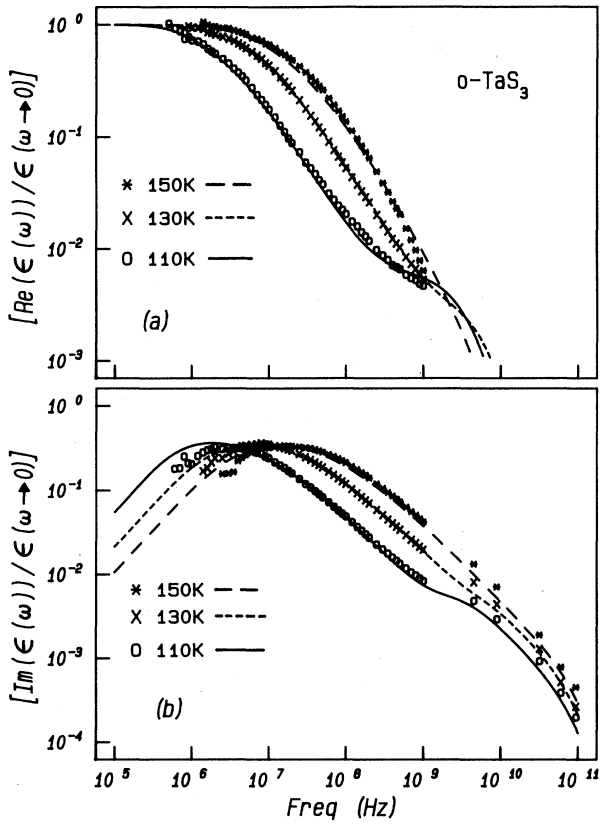

FIG. 2. Dielectric response of o-TaS_3 normalized to the measured static dielectric constant $\epsilon(\omega\rightarrow 0)$. Data points and theory curves are both calculated from the ac conductivity shown in Fig. 1. Values of $\epsilon(\omega\rightarrow 0)$ are plotted in Fig. 4.

dielectric relaxation frequency, as measured by the peak in Im(ϵ) and plotted in Fig. 3, shifts to dramatically lower frequencies in an Arrhenius manner. In addition, the magnitude of the static dielectric constant is found to increase by a factor of $\sim$3 from 150 to 100 K, as illustrated in Fig. 4. The results shown in Fig. 1 clearly demonstrate that the change in $\sigma(\omega)$ observed below 150 K is not due to increasing disorder, as previously reported,[15] but instead results from the dominance of a second mode at millimeter-wave frequencies and the appearance of a temperature-activated response at rf frequencies.

The form that we have used to model the measured CDW ac conductivity is given by

$$\sigma(\omega)=\frac{n_c e^2}{M_F}\left[\frac{1}{\tau_i}+\frac{\omega_p^2}{i\omega}+i\omega+\frac{1}{\tau_A+\frac{i\omega}{(\omega_p')^2}}\right]^{-1}. \quad (2)$$

This model can also be represented by the equivalent electrical circuit shown in the inset of Fig. 3. Parameters given in Table I were used to compute the curves shown in Figs. 1 and 2. At lower temperatures, where the measured rf response is temperature activated, two CDW

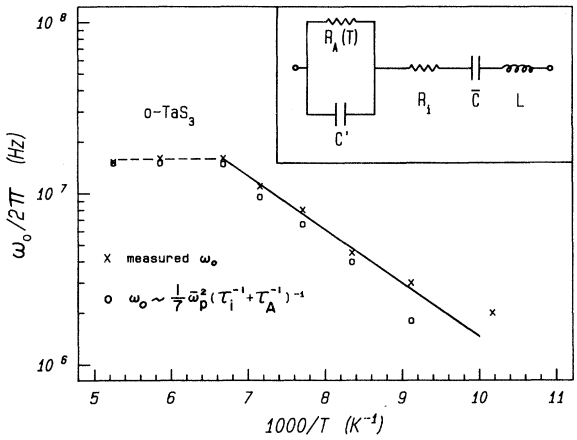

FIG. 3. Dielectric relaxation frequency ω_0 vs inverse temperature. Measured (×) values are taken from the peak in Im[$\epsilon(\omega)$]. Calculated (○) values are based on the expression shown in the figure, which simplifies at low temperature to $\omega_0 \approx \bar{\omega}_p^2 \tau_A/7 \approx \beta\sigma_n/\epsilon(\omega\rightarrow 0)$ with $\beta \sim 12$. Below 150 K the activation energy is ~720 K (solid line). The dashed line is a guide to the eye. The inset shows an electrical circuit equivalent to Eq. (2). Correspondence between circuit elements and the model is indicated in Table I.

pinning frequencies and their associated damping constants are clearly needed. At higher temperatures, only the lower pinning frequency effectively appears. This lower pinning frequency ω_p corresponds to the average phase correlation length L, and therefore has a distribution associated with it at all temperatures. The total ac conductivity is obtained by convolving this distribution for ω_p with the expression given in Eq. (2). The distribution function that we have used is based upon a random

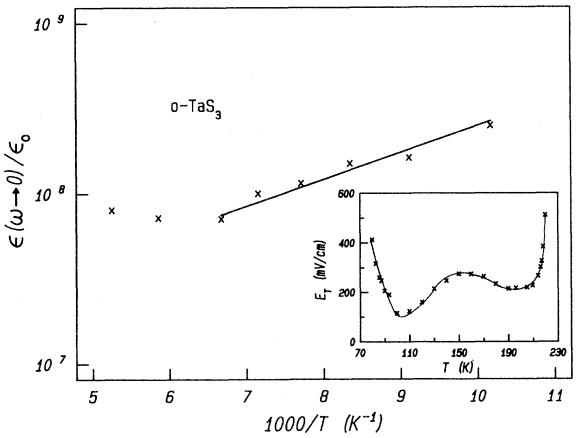

FIG. 4. Measured values of the static CDW dielectric constant $\epsilon(\omega\rightarrow 0)$ vs inverse temperature. $\epsilon(\omega\rightarrow 0)$ is temperature activated from 150 to 100 K (solid line) with an activation energy of ~350 K. The inset shows the measured dc threshold field E_T. Note the decrease in E_T from 150 to 100 K.

TABLE I. Parameters for o-TaS_3 used in model calculations. Correspondence to equivalent electrical model, shown in Fig. 3, is indicated above each column heading; in addition, $M_F/n_c e^2 \leftrightarrow L$.

	$\omega_p' \leftrightarrow \frac{1}{(LC')^{1/2}}$	$\frac{1}{\tau_i} \leftrightarrow \frac{R_i}{L}$	$\bar{\omega}_p \leftrightarrow \frac{1}{(L\bar{C})^{1/2}}$	$\frac{1}{\tau_A} \leftrightarrow \frac{R_A}{L}$
T	$\frac{\omega_p'}{2\pi}$	$\frac{1}{2\pi\tau_i}$	$\frac{\bar{\omega}_p}{2\pi}$	$\frac{1}{2\pi\tau_A}$
(K)	(GHz)	(GHz)	(GHz)	(GHz)
150	16	100	3.3	5[a]
130	15	100	2.8	70
110	14	100	2.1	250

[a] $1/2\pi\tau_A < 5$ GHz reproduces a single oscillator response with a distribution.

variation in the phase correlation length l given by $P(l) = L^{-1}\exp(-l/L)$. This yields the corresponding distribution in pinning frequencies $P(\omega_p) = (\bar{\omega}_p/\omega_p^2)\exp(-\bar{\omega}_p/\omega_p)$, based on the relation $\omega_p = \pi c_0/l$ with c_0 the unpinned CDW phason velocity.[9] Here, $\bar{\omega}_p = \pi c_0/L$ represents the average pinning frequency for these large-volume average phase modes.

The average pinning frequency $\bar{\omega}_p$ in Table I has been calculated from the measured values of $\epsilon(\omega\rightarrow 0)$, using Eq. (1) and the estimates $n_c \approx 6\times 10^{21}$ cm^{-3} and $M_F \approx 1000 m_e$ for o-TaS_3. The intrinsic CDW damping parameter $1/\tau_i$ has been obtained from the measured rolloff in ac conductivity within the millimeter-wave region.[14] The additional temperature-activated damping $1/\tau_A$ of the large-volume average phase modes, due to restricted normal carrier screening, becomes important below 150 K. Well into this region, we can estimate the damping parameter using the measured dielectric relaxation frequency and the relation $\omega_o \approx \bar{\omega}_p^2 \tau_A/7$. Here the numerical factor of ~7 enters only because of the broad distribution about the average pinning frequency. This relation yields an Arrhenius form for the damping, since the dielectric relaxation frequency $\omega_o \approx \sigma_n(T)/\epsilon(\omega\rightarrow 0)$ is seen to be temperature activated for $T < 150$ K in Fig. 3. Figure 1 also shows a successive transfer of oscillator strength into the millimeter-wave mode at $\omega_p'/2\pi \approx 15$ GHz as the lower-frequency modes are frozen out. This value of ω_p' is consistent with our previous theoretical estimates for the coherent oscillation frequency of the CDW on the volume scale n_i^{-1} surrounding each impurity site.[10,11]

The results displayed in Figs. 1 and 2 illustrate universal features of the rf conductivity and dielectric response for a pinned CDW. Data taken on $NbSe_3$ show no temperature-activated region[13] due to the additional screening provided by partially filled normal carrier bands. This temperature-independent behavior is also seen above 150 K in o-TaS_3, where only the average phase modes contribute to the ac conductivity. Results strikingly similar to the o-TaS_3 data below 150 K have also been obtained for $K_{0.30}MoO_3$, $(TaSe_4)_2I$, and $(NbSe_4)_{10/3}I$,[5,16–18] where the ac low-frequency conduc-

tivity is temperature activated and the presence of a single additional mode at millimeter-wave frequencies is apparent. The phenomenological model described by Eq. (2) and illustrated in Fig. 3 therefore closely reproduces the complete ac dynamics of a pinned CDW in this portion of the spectrum, using a few simple parameters, $\epsilon(\omega\rightarrow 0)$, $1/2\pi\tau_i$, and $\sigma_n(T)$, obtained directly from experiment.

Finally, the static dielectric constant $\epsilon(\omega\rightarrow 0)$ is found to increase slowly in o-TaS_3 between 150 and 100 K in a quasiactivated manner, as shown in Fig. 4. This effect is reminiscent of the activated increase in $\epsilon(\omega\rightarrow 0)$ for $K_{0.30}MoO_3$ seen previously between 100 and 60 K.[5] The CDW is known to become nearly commensurate in both o-TaS_3 and $K_{0.30}MoO_3$ below approximately 130 and 100 K, respectively.[19,20] We propose that in each of these materials the average longitudinal phase correlation length L increases due to the approach toward commensurability, causing $\epsilon(\omega\rightarrow 0)$ to increase and the dc threshold field E_T to decrease over a limited temperature range.[21] This is in sharp contrast to the dramatic decrease in the phase correlation length that would be expected for a true lock-in to commensurate pinning. The apparent absence of a lock-in despite the nearly commensurate value of the CDW wave vector can be explained by the relative phasing of the CDW chains in the transverse directions within the unit cell.[2] Because of this relative phasing, it is possible to have zero net gain in commensurate pinning energy (CPE), so that the pinning remains dominated by impurities despite a commensurate CDW wave vector. NMR line shapes in $Rb_{0.30}MoO_3$ at temperatures as low as 40 K clearly show an incommensurate CDW structure although λ_{CDW} is essentially commensurate.[22] In addition, the *decrease* of the dc threshold field E_T below the supposed lock-in transitions for $K_{0.30}MoO_3$ and o-TaS_3 is clear evidence against any *additional* sources of pinning (i.e., commensurability) entering at low temperature.

In a CDW material with strong impurity pinning, a sufficiently large CPE on the *individual* chains within the unit cell can make it highly unfavorable for the phase of the CDW to be pinned at a particular impurity site in an "anticommensurate" configuration. The CPE can thus act to overcome the impurity pinning energy and effectively eliminate a significant fraction of the pinning sites, with a corresponding increase in the phase correlation length L and reduction in the threshold field. More impurity sites should be effectively removed at lower temperatures, as the system approaches an exactly commensurate wave vector. The increase towards commensurability in $K_{0.30}MoO_3$ of the CDW's wave vector has been explained as the thermal depopulation of an additional midzone band,[23] providing a mechanism for the temperature-activated increase in $\epsilon(\omega\rightarrow 0)$ and decrease in dc threshold field E_T. The inset of Fig. 4 verifies that E_T also decreases in o-TaS_3, by a factor of ~ 2 from 150 to 100 K. Within our strong-pinning model,[10] the observed factor-of-3 increase in $\epsilon(\omega\rightarrow 0)$ should result in a factor of $\sim\sqrt{3}$ increase in the phase correlation length L and a $(\sqrt{3})^{4/3}\sim 2$ decrease in E_T, as observed. Similar rough numerical agreement is obtained for the behavior of $\epsilon(\omega\rightarrow 0)$ and E_T in $K_{0.30}MoO_3$.[24]

ACKNOWLEDGMENTS

This work was supported by the National Science Foundation (under Grant No. NSF-DMR-87-15431) and by the U.S. Joint Services Electronics Program (under Contract No. N00014-84-C-0149).

[1] G. Grüner and A. Zettl, Phys. Rep. **119**, 117 (1985).
[2] P. Monceau, in *Electronic Properties of Inorganic Quasi-One-Dimensional Compounds,* edited by P. Monceau (Riedel, Dordrecht, 1985).
[3] G. Grüner, A. Zawadowski, and P. Chaikin, Phys. Rev. Lett. **46**, 511 (1981); P. Monceau, J. Richard, and M. Renard, Phys. Rev. B **25**, 931 (1982).
[4] S. Sridhar, D. Reagor, and G. Grüner, Phys. Rev. Lett. **55**, 1196 (1985).
[5] R. J. Cava, R. M. Fleming, P. Littlewood, E. A. Rietman, L. F. Schneemeyer, and R. G. Dunn, Phys. Rev. B **30**, 3228 (1984).
[6] J. P. Stokes, M. O. Robbins, and S. Bhattacharya, Phys. Rev. B **32**, 6939 (1985).
[7] R. J. Cava, R. M. Fleming, R. G. Dunn, E. A. Rietman, and L. F. Schneemeyer, Phys. Rev. B **30**, 7290 (1984).
[8] R. J. Cava, R. M. Fleming, R. G. Dunn, and E. A. Rietman, Phys. Rev. B **31**, 8325 (1985).
[9] H. Fukuyama and P. A. Lee, Phys. Rev. B **17**, 535 (1978); P. A. Lee and T. M. Rice, *ibid.* **19**, 3970 (1979).
[10] J. R. Tucker, W. G. Lyons, and G. Gammie, Phys. Rev. B **38**, 1148 (1988).
[11] W. G. Lyons and J. R. Tucker, Phys. Rev. B **38**, 4303 (1988).
[12] R. J. Cava, P. B. Littlewood, R. M. Fleming, L. F. Schneemeyer, and E. A. Rietman, Phys. Rev. B **34**, 1184 (1986).
[13] W.-Y. Wu, L. Mihaly, G. Mozurkewich, and G. Grüner, Phys. Rev. B **33**, 2444 (1986).
[14] S. Sridhar, D. Reagor, and G. Grüner, Phys. Rev. B **34**, 2223 (1986).
[15] A. Zettl, C. M. Jackson, and G. Grüner, Phys. Rev. B **26**, 5773 (1982).
[16] J. R. Tucker, W. G. Lyons, J. H. Miller, Jr., R. E. Thorne, and J. W. Lyding, Phys. Rev. B **34**, 9038 (1986).
[17] R. J. Cava, P. Littlewood, R. M. Fleming, R. G. Dunn, and E. A. Rietman, Phys. Rev. B **33**, 2439 (1986).
[18] T. Sekine, T. Tsuchiya, and E. Matsuura, in *Physics and Chemistry of Quasi One-Dimensional Conductors,* Proceedings of the Yamada Conference XV, edited by S. Tanaka and K. Uchinokura (North-Holland, Amsterdam, 1986), p. 158 [Physica B+C **143B**, 158 (1986)].
[19] Z. Z. Wang, H. Salva, P. Monceau, M. Renard, C. Roucau, R. Ayroles, F. Levy, L. Guemas, and A. Meerchaut, J. Phys. (Paris) Lett. **44**, L311 (1983).
[20] R. M. Fleming, L. F. Schneemeyer, and D. E. Moncton, Phys.

Rev. B **31**, 899 (1985).
[21]In o-TaS_3 *below* 100 K, the increase in ω_p' seen in Ref. 14 and rapid rise in E_T may well be indications of a commensurate lock in.
[22]K. Nomura, K. Kume, and M. Sato, Solid State Commun. **57**, 611 (1986); A. Janossy, C. Berthier, P. Segransan, and P. Butaud, Phys. Rev. Lett. **59**, 2348 (1987).
[23]J. P. Pouget, C. Noguera, A. H. Moudden, and T. J. Moret, J. Phys. (Paris) **46**, 1731 (1985).
[24]J. R. Tucker and W. G. Lyons, Phys. Rev. B **38**, 7854 (1988).